Flash Photolysis–Resonance Fluorescence Kinetic Study of the Reactions OH + H_2 → H_2O + H and OH + CH_4 → H_2O + CH_3 from 298 to 1020 K

F. P. Tully† and A. R. Ravishankara*

Molecular Sciences Branch, Engineering Experiment Station, Georgia Institute of Technology, Atlanta, Georgia 30332
(Received: March 27, 1980; In Final Form: July 16, 1980)

Absolute rate constants for the reactions OH + H_2 → H_2O + H (k_1) and OH + CH_4 → H_2O + CH_3 (k_2) have been measured between 298 and 1020 K by using the flash photolysis–resonance fluorescence technique. These measurements represent the first use of this technique in kinetic studies of radial–molecule reactions above 500 K. The obtained $k_1(T)$ and $k_2(T)$ values clearly demonstrate the existence of curvature in the Arrhenius graphs for the subject reactions. These data are compared with those of previous experiments and data evaluations on reactions 1 and 2.

Introduction

Experimental measurements of absolute rate constants for radical–molecule reactions have historically been divided according to temperature regime. At low temperature ($T \lesssim 500$ K) a variety of techniques[1] have been developed and utilized in recent years in response to the input demands of atmospheric chemical modeling. Generally speaking these techniques permit the adjustment of experimental conditions such that the absolute rate-constant measurements for many specific radical–molecule reactions may be made with little, and/or quantifiable, interference from competing reaction processes. At high temperature ($T \gtrsim 1000$ K) kinetic isolation of a given reaction has proved to be much more difficult to achieve. Experiments at flame temperatures typically range from studies utilizing end-product analysis alone to investigations involving detailed concentration mapping vs. time (distance) of a number of radical (stable molecule) species whose interactive chemistry is very complex. Sequences of reaction schemes with parameterized absolute rate-constant values are used to iteratively reproduce the measured concentration profiles (product yields). Frequently the extracted rate constants are model dependent, ratioed to those of other insufficiently characterized reactions, or sensitive within only broad limits on the obtained raw data. The interpretive clarity of high-temperature kinetic measurements has been observed to parallel the level of experimental control.

At temperatures intermediate between these separated regimes, 500–1000 K, relatively few investigations of radical–molecule reaction rate constants have been undertaken. Two reactions (eq 1 and 2) which have recieved

$$OH + H_2 \xrightarrow{k_1} H_2O + H \qquad (1)$$

$$OH + CH_4 \xrightarrow{k_2} H_2O + CH_3 \qquad (2)$$

some attention[2,3] in this interval as well as extensive study at high and low temperatures are the subject of the present investigation. Published kinetic data on reaction 1 has recently been critically evaluated and summarized by Cohen and Westberg.[4] Principally on the basis of kinetic measurements made below 500 K and above 1000 K, these authors recommended a three-parameter, rate-constant expression of functional form $k(T) = AT^n \exp(-E_0/RT)$ as an appropriate fit to the Arrhenius graph curvature experimentally defined for reaction 1. Non-Arrhenius behavior is also evident in kinetic measurements made on reaction 2. Zellner[5] has used this same functional form to empirically effect a smooth joining of the low- and high-temperature rate-constant measurements for this reaction.

In this paper we present the first in a series of studies of the reaction kinetics of the hydroxyl radical at intermediate temperatures. Using the direct kinetic technique of flash photolysis–resonance fluorescence we have obtained absolute rate constants for reactions 1 and 2 up to temperatures of 1000 K. These results will be described and compared with those of previous measurements and compilations.

Experimental Section

The application of the flash photolysis–resonance fluorescence technique to the study of OH radical reaction kinetics has been discussed previously.[6] Hence we will describe the experimental apparatus briefly, emphasizing only those new features which for the first time extend the temperature range of applicability of the technique to above 1000 K.

A schematic diagram of the experimental apparatus is shown in Figure 1. The principal components of this system are (1) a quartz reaction cell resistively heated by using electrically insulated tantalum wire windings mounted to its graphite-coated outer surface, (2) a spark discharge flash lamp perpendicular to one face of the cell, (3) a CW OH resonance lamp perpendicular to the photolysis beam, (4) a photomultiplier/band-pass filter combination for monitoring OH resonance fluorescence perpendicular to both the photolysis and resonance radiation beams, and (5) a signal averager and fast photon counting electronics.

The present experiments were carried out by using a static reactor configuration. Typical gas mixtures consisting of 150 mtorr of H_2O, 0–1 torr of $H_2(CH_4)$, and 50 torr of argon were flash photolyzed, thereby initiating the primary reaction sequence

$$H_2O \xrightarrow[165 < \lambda < 185\ nm]{h\nu} H + OH(X^2\Pi)$$

$$OH + H_2(CH_4) \xrightarrow{k_{bi}} H_2O + H(CH_3)$$

It is worth noting here that our use of Suprasil quartz optics with a transmission cutoff at 165 nm prevented photolysis of H_2 and CH_4[7] and thus eliminated a major potential source of unwanted radicals and competing

† Applied Physics Division, Sandia National Laboratories, Livermore, California 94550.

0022-3654/80/2084-3126$01.00/0

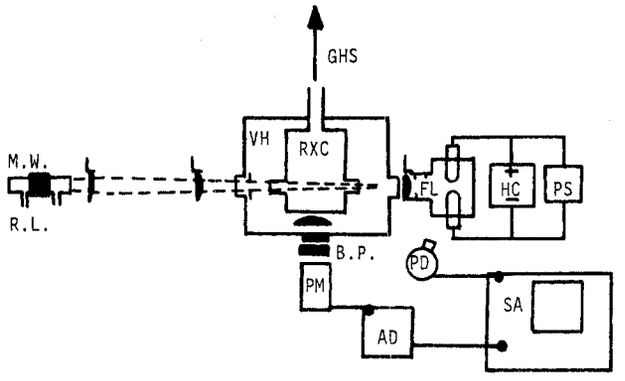

AD: AMPLIFIER/DISCRIMINATOR
B.P.: BANDPASS FILTER
FL: FLASHLAMP
GHS: GAS HANDLING SYSTEM
HC: HIGH VOLTAGE CAPACITOR
L: LENS
M.W.: MICROWAVE CAVITY (Evenson Type)
PD: PHOTODIODE
PM: PHOTOMULTIPLIER
PS: POWER SUPPLY
R.L.: RESONANCE LAMP
RXC: REACTION CELL
VH: VACUUM HOUSING
SA: SIGNAL AVERAGER

Figure 1. Schematic drawing of the experimental apparatus. (For clarity the flash lamp and the resonance lamp are pictured at 180° to each other, whereas in reality they were situated at 90°).

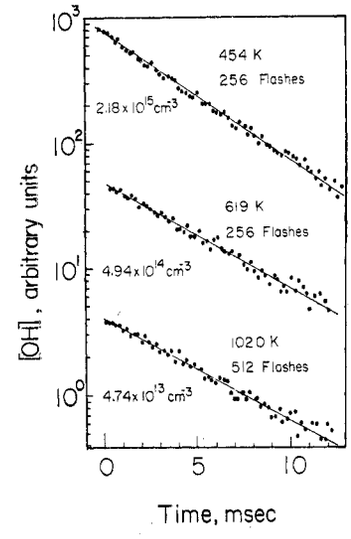

Figure 2. Typical OH temporal profiles observed following flash photolysis of H_2O/CH_4/diluent mixtures. Experimental conditions: $P = 50$ torr, diluent = Ar, flash energy = 120 J, H_2O pressure = 150 mtorr. The concentrations of methane, the temperature, and the number of traces averaged are shown next to each line.

radical–radical reaction processes. Following the flash weakly focused resonance lamp radiation continuously exicted a small fraction of the OH to the $A^2\Sigma^+$ state, and the resultant (0,0) band fluorescence was counted in real time; the temporal profile of OH decay was constructed by signal averaging over a large number of flashes for each fixed reactant concentration. The reactant concentrations $[H_2]$ and $[CH_4]$ were maintained at large excess over [OH] ($[OH]_{t=0} \approx 1 \times 10^{11}$–$5 \times 10^{11}$ molecules/cm^3), and the reaction kinetics were thus pseudo first order in [OH]. Exponential [OH] decays (through several $1/e$ times) were obtained, their time constants yielding the first-order rate constant for OH disappearance at the reactant concentration of that mixture. Bimolecular rate constants were obtained as the slope of a plot of the measured first-order rate constant vs. reactant concentration ($[H_2]$ or $[CH_4]$). System parameters such as flash energy, H_2O concentration, and total pressure were varied to demonstrate the lack of importance of competing secondary processes in our measurements on reactions 1 and 2. During the generation of most [OH] decay curves, several cycles of reactor filling/evacuation with identical gas mixtures were used so as to negate the kinetically deleterious effects of reactant depletion and product buildup (within the exposure limits used the measured rate constants were shown to be independent of the number of flashes to which any gas filling was subjected).

The two principal experimental factors which have permitted direct measurements of absolute rate constants to be made at temperatures in excess of 1000 K involve the system optics configuration and the reaction cell design. Collimation and weak focusing of the incoming flash lamp and resonance lamp radiation and of the emitted fluorescence have been employed and have resulted in an OH detection sensitivity which is significantly enhanced relative to that available in previous high-pressure studies of reactions 1 and 2. A detailed discussion of the detection sensitivity characteristics of a completely analogous experimental configuration is contained in a recent publication[8] describing our laboratory's study of the OH + NO_2 + M → HNO_3 + M reaction. Highly polished Suprasil windows have been fused by using quartz tape to an all-quartz body to form the high-temperature reactor.[9] Efficient heating and radiation shielding maintain a higher temperature at the body of the reactor than that at the protruding windows, the reaction temperature being measured by both internal (insertable) and external (body-mounted) chromel–alumel thermocouples. During the period of measurement of each individual bimolecular rate constant, the reactor temperature was held constant to within ±3 K by applying a controlled constant voltage to the resistive heaters. The temperature profile along the axis of the cylindrical reactor was measured by using the retractable thermocouple at pressure conditions identical with those existing during kinetic measurements. The temperature differential between the upper and lower portions of the reaction zone (maximum length ≈ 2 cm) was found to be ≤5 K at a reactor temperature of 1000 K. The bottom window (fluorescence port) temperature was measured to be ≈25 K below that of the reaction zone at 1000 K; given the heater and radiation shield positions and the overall reactor geometry, side window temperatures are estimated to be comparable to that measured at the bottom window. Considering the relatively large reactor diameter used in this work (reactor volume ≈ 500 cm^3), such temperature gradients are likely to be only a minimal source of experimental error.

Figure 2 shows typical OH decay profiles at three temperatures. These decay rates were all measured by using the same diluent gas pressure, H_2O pressure, and photolysis flux. the high-temperature experiments required longer periods of signal averaging than the lower-temperature measurements; for example, twice as many flashes were needed at 1020 K than at 619 K to produce a good quality decay curve. At an H_2O partial pressure of ~150 mtorr, the fluorescence signal strength as a function of temperature was seen to scale closely with H_2O number density, indicating minimal temperature-dependent optics transmission effects; repeated temperature cycling of the reactor did, however, induce long-term degradation of the vacuum-UV transmission efficiency of the Suprasil windows. (The static reactor used in the present work has since been replaced by an analogous "slow flow" high-temperature quartz reaction cell which transmits a continuously controlled flow of mixture of desired composition

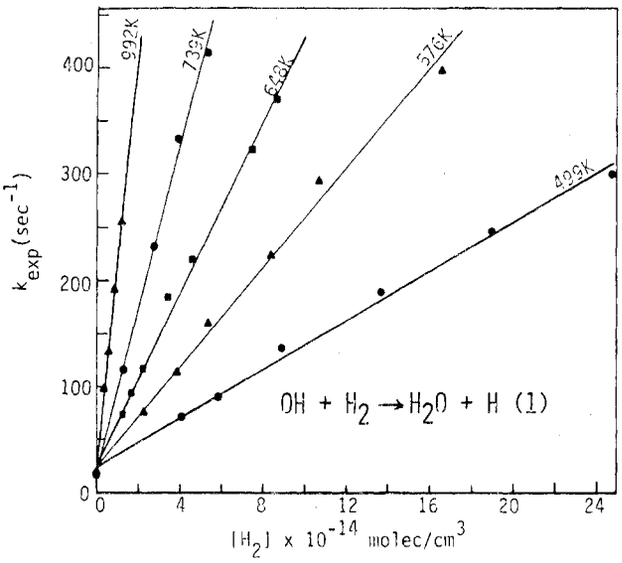

Figure 3. Plot of the first-order rate constant vs. the H_2 concentration for reaction 1 at several temperatures.

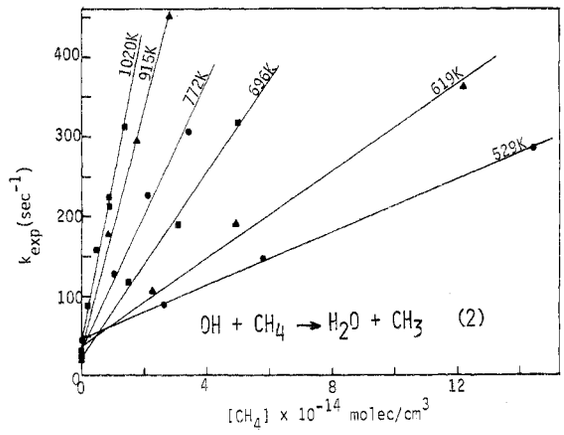

Figure 4. Plot of the first-order rate constant vs. the CH_4 concentration for reaction 2 at several temperatures.

and thereby permits each initiating flash to encounter a "locally fresh" reaction mixture.)

The gases used in this study were obtained from Matheson Co. and had stated minimum purities as follows: H_2, 99.9999%; CH_4, 99.99%; and Ar, 99.9995%. Before their use, hydrogen and methane were passed through a trap at 77 K to remove residual condensibles.

Results and Discussion

The bimolecular reaction rate constants obtained in this study were generated from measurements of hydroxyl radical decay rates at several fixed reactant concentrations for each temperature. Plots of the first-order decay constant vs. reactant concentration at selected temperatures between 499 and 1020 K are given for reactions 1 and 2 in Figures 3 and 4, respectively. The bimolecular rate constants obtained as the slopes of the included least-squares lines are listed with $\pm 2\sigma$ precision limits in Tables I and II. Room-temperature rate-constant values obtained in this work are in good agreement with those of previous studies tabulated in the data evaluations of ref 4 and 5.

The major potential sources of systematic error in the measured values of k_1 and k_2 are the uncertainties in the reactant concentrations and in the temperature. At 298 K the reactant concentrations of source mixtures could be determined quite accurately (≈3%) by using a capacitance manometer since both H_2 and CH_4 are nonsticky and

TABLE I: Bimolecular Rate Constant vs. Temperature for Reaction 1: OH + H_2 → H_2O + H

temp, K	$k_{bimolecular}$,[a] cm^3 molecule^{-1} s^{-1}
298	(6.08 ± 0.37) × 10^{-15}
499	(1.15 ± 0.08) × 10^{-13}
576	(2.34 ± 0.18) × 10^{-13}
648	(3.84 ± 0.18) × 10^{-13}
739	(7.64 ± 0.56) × 10^{-13}
838	(1.30 ± 0.10) × 10^{-12}
904	(1.86 ± 0.35) × 10^{-12}
992	(1.99 ± 0.19) × 10^{-12}

[a] Stated error bounds represent the 2σ values.

TABLE II: Bimolecular Rate Constant vs. Temperature for Reaction 2: OH + CH_4 → H_2O + CH_3

temp, K	$k_{bimolecular}$,[a] cm^3 molecule^{-1} s^{-1}
298	(7.50 ± 0.60) × 10^{-15}
398	(4.73 ± 0.45) × 10^{-14}
448	(8.1 ± 1.1) × 10^{-14}
511	(1.45 ± 0.12) × 10^{-13}
529	(1.67 ± 0.06) × 10^{-13}
600	(3.14 ± 0.40) × 10^{-13}
619	(2.75 ± 0.44) × 10^{-13}
696	(5.78 ± 0.58) × 10^{-13}
772	(8.4 ± 1.5) × 10^{-13}
915	(1.50 ± 0.15) × 10^{-12}
1020	(2.00 ± 0.20) × 10^{-12}

[a] Stated error bounds represent the 2σ values.

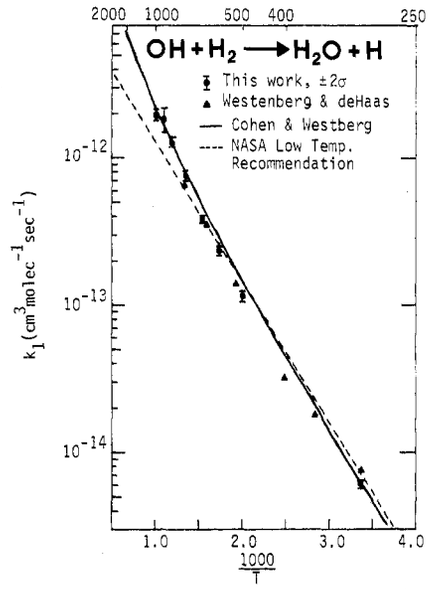

Figure 5. Arrhenius graph for reaction 1.

noncondensible compounds. Reaction fillings were made by using these calibrated source mixtures, and elevated temperature reactant concentrations were calculated by scaling accordingly to source mixture content and temperature. Including errors due to temperature uncertainties, then, the estimated error in reactant concentrations was ≤10%. Thus we estimate that the accuracies (95% confidence limit) of the measured values of k_1 and k_2 are ~13% at 298 K increasing to ~20% at 1000 K.

Our data for $k_1(T)$ are plotted along with selected previous results and analytical evaluations in Arrhenius graph form, ln $k(T)$ vs. $1000/T$, in Figure 5. Our results cover a sufficiently wide temperature range to independently demonstrate the existence of curvature in the Arrhenius plot for reaction 1. At low and relatively high temperature our measurements are in excellent agreement with the

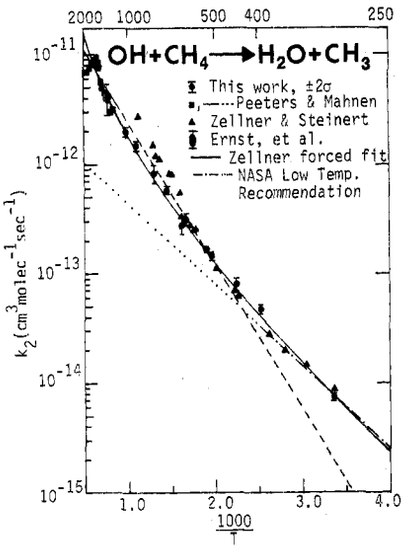

Figure 6. Arrhenius graph for reaction 2.

rate-constant values calculated from Cohen and Westberg's summary expression[4] ($k_1(T) = 1.83 \times 10^{-15}T^{1.3} \cdot \exp(-1835/T)$ cm^3 molecule^{-1} s^{-1}). In the interval 499–648 K, however, measurements made in the present study fall ~20% below those derived from this $k_1(T)$ expression. Similarly, in the only previously published direct kinetic study of reaction 1 at intermediate temperatures, Westenberg and deHaas[2] measured k_1 values between 403 and 745 K which averaged 22% below those calculated from the Cohen and Westberg formula. Interestingly Cohen and Westberg did not weight data at intermediate temperatures heavily in their evaluation; indeed, hardly any measurements between 500 and 1000 K were available. While our measurements yield generally very good agreement with the $k_1(T)$ values calculated from Cohen and Westberg's expression, they do suggest somewhat more pronounced Arrhenius graph curvature than that expression describes. The best-fit expression calculated from our data only is $k_1(T) = 4.12 \times 10^{-19}T^{2.44} \exp(-1281/T)$ cm^3 molecule^{-1} s^{-1}. Zellner's suggested[5] expression of $k_1(T) = 1.66 \times 10^{-16}T^{1.6} \cdot \exp(-1660/T)$ cm^3 molecule^{-1} s^{-1} is perhaps the most appropriate fit to all available data. (With regard to curvature in Arrhenius plots, it is of interest to note that preliminary results of our OH + D_2 → DHO + D study[10] between 298 and 932 K demonstrate markedly less Arrhenius graph curvature than that found to be appropriate for reaction 1.)

Our rate-constant measurements for the OH + CH_4 → H_2O + CH_3 reaction are plotted along with selected previous work in Arrhenius graph form in Figure 6. Once again our data clearly demonstrate the existence of pronounced Arrhenius graph curvature for reaction 2. Immediately apparent from this figure is the fact that straight-line extrapolations of either the low-temperature-based NASA recommendation[11] or the high-temperature-based Peeters and Mahnen recommendation[12] produce order of magnitude errors in $k_2(T)$ in the opposite temperature regime. On the basis of principally low- and high-temperature experimental measurements, Zellner[5] derived an empirical best fit for $k_2(T)$ given by $k_2(T) = 2.57 \times 10^{-18}T^{2.13} \exp(-1233/T)$ cm^3 molecule^{-1} s^{-1}. Within experimental error both our data (298–1020 K) and the single point of Ernst, Wagner, and Zellner (1300 K)[13] fall dead on the curve (solid line in Figure 6) traced out by this expression. Interestingly, the calculated best-fit expression based on our data only, $k_2(T) = 1.32 \times 10^{-17}T^{1.92} \cdot \exp(-1355/T)$ cm^3 molecule^{-1} s^{-1}, yields a curve which is barely distinguisable from the recommended by Zellner. Indeed, given the quoted accuracies of these and previous measurements on reaction 2, a rather extended array of parameters could be suggested as producing representative fits for $k_2(T)$. While the present experiments have demonstrated both the appropriateness of the functional form $k(T) = AT^n \exp(-E_0/RT)$ and the basic soundness of previous measurements in each separated temperature regime, the curve-fitting calculations indicate that extreme caution must be exercised when attaching physical significance to multiparameterized rate-constant expressions.

At intermediate temperatures only one prior direct kinetic investigation of reaction 2 has been undertaken. Using the technique of flash photolysis–resonance absorption, Zellner and Steinert[3] measured $k_2(T)$ up to temperatures of 892 K. At lower temperatures these data agree well with Zellner's empirical fit, but at higher temperatures their measured $k_2(T)$ values exceed the best-fit values by a factor increasing with temperature and already more than 2 at 892 K.

One possible explanation for the discrepancy at higher temperatures between Zellner and Steinert's results and those of the present study relates to the magnitude of the hydroxyl radical reactant concentration demanded by the resonance absorption and fluorescence detection modes. Although both techniques measure the disappearance of OH radicals in real time, the absorption technique monitors the difference between two large numbers ($(I_{t=0} - I_t)/I_{t=0}$) and thereby requires much larger OH concentrations to match the statistics obtainable from the fluorescence technique. Thus Zellner and Steinert's initial postflash OH concentrations were 40–100 times higher and their $[CH_4]/[OH]_{t=0}$ ratios were ~10 times lower than those characteristic of the present study. Such larger radical concentrations and lower reactant ratios enhance the probability of OH disappearance due to processes other than reaction 2 and make more difficult kinetic isolation of this subject reaction. Based on sensitivity considerations, then, it appears that the fluorescence detection technique is best suited to the investigation of intermediate-temperature hydroxyl radical reaction kinetics; indeed, it is the authors' opinion that present constraints on the general applicability of the flash photolysis–resonance fluorescence technique to combustion regime kinetics of O, H, and OH relate more to maintenance of the mechanical and optical integrity of the experimental system than to limitations in detection sensitivity.

The experiments described above represent the first use of the flash photolysis–resonance fluorescence technique in the study of radical–molecule reaction kinetics above 500 K. The need for direct kinetic investigations of prototype radical–molecule reactions from low temperatures to those well within the flame region is indisputable. Combustion modeling requires voluminous rate-constant input from both direct measurement and extrapolation (note here the improvement in extrapolative accuracy achievable upon progression of data availability limits from 400 K ($1000/T = 2.5$) to 1000 K ($1000/T = 1.0$)). Enhancement of our general understanding of bimolecular reaction rate theory is ultimately required to render practical the global kinetic approach to the chemical modeling of complex systems. Umambiguous rate-constant studies over wide temperature ranges ($0.5 \leq 1000/T \leq 5.0$) will promote this goal.

Acknowledgment. This work was supported by the Air Force Office of Scientific Research under Contract No. F49620-77-C-0111. Early stages of the apparatus-development phase of this work were supported by the National

Bureau of Standards through Grant No. GT-9020.

References and Notes

(1) (a) C. J. Howard, *J. Phys. Chem.*, **83**, 3 (1979); (b) J. V. Michael and J. H. Lee, *ibid.*, **83**, 10 (1979); (c) F. Kaufman, *Annu. Rev. Phys. Chem.*, **30**, 411 (1979), and references therein.
(2) A. A. Westenberg and N. deHaas, *J. Chem. Phys.*, **58**, 4061 (1973).
(3) R. Zellner and W. Steinert, *Int. J. Chem. Kinet.*, **8**, 397 (1976).
(4) N. Cohen and K. Westberg, *J. Phys. Chem.*, **83**, 46 (1979).
(5) R. Zellner, *J. Phys. Chem.*, **83**, 18 (1979).
(6) (a) D. D. Davis, S. Fischer, and R. Schiff, *J. Chem. Phys.*, **59**, 628 (1974); (b) A. R. Ravishankara, P. H. Wine, and A. O. Langford, *ibid.*, **70**, 984 (1979), and references therein.
(7) J. G. Calvert and J. N. Pitts, Jr., "Photochemistry", Wiley, New York, 1966.
(8) P. H. Wine, N. M. Kreutter, and A. R. Ravishankara, *J. Phys. Chem.*, **83**, 3191 (1979).
(9) The reactor was fabricated by R and D Opticals, Inc., New Windsor, MD.
(10) A. R. Ravishankara, R. C. Shah, J. M. Nicovich, R. L. Thompson, and F. P. Tully, work in progress.
(11) R. D. Hudson and E. I. Reed, "The Stratosphere: Present and Future", *NASA Ref. Publ.*, **1049**, Dec 1979.
(12) J. Peeters and G. Mahnen, *Symp. (Int.) Combust., [Proc.]*, **14**, 133 (1973).
(13) J. Ernst, H. Gg. Wagner, and R. Zellner, *Ber. Bunsenges. Phys. Chem.*, **82**, 409 (1978).

Raman Spectra of Methanol and Ethanol at Pressures up to 100 kbar

J. F. Mammone,* S. K. Sharma,

Geophysical Laboratory, Carnegie Institution of Washington, Washington, D.C. 20008

and M. Nicol

Department of Chemistry, University of California, Los Angeles, California 90024 *(Received: April 7, 1980)*

The Raman spectra of methanol and ethanol were measured at pressures up to 100 kbar and room temperature. At these pressures methanol either crystallizes or forms a glass (superpressed liquid), whereas ethanol always crystallizes. The pressure at which methanol crystallizes is estimated to be 35.1 ± 1.0 kbar. Comparison of the Raman spectrum of high-pressure crystals with that of the low-temperature α-methanol indicates that the structure of the high-pressure phase resembles that of the α phase. The Raman spectra for ethanol, which crystallized at 17.8 ± 1.0 kbar, were interpreted in terms of the monocliniic (Pc; $Z = 4$) low-temperature structure. In ethanol, the frequency of the O–H stretching modes shows large negative shifts with pressure due to the strengthening of the hydrogen bonds.

Introduction

At 1 atm methanol freezes at 175 K and undergoes a λ transition[1] at 161 K; ethanol freezes[2] at 156 K. Vibrational spectra of the solid low-temperature forms of methanol have been extensively studied by infrared[3-5] and Raman[5] spectroscopy. Polarized infrared spectra of single crystals of ethanol at room temperature have been measured in a diamond-window, high-pressure cell.[6]

The nature of the intermolecular forces in these hydrogen-bonded systems not only is of fundamental theoretical interest[1,7] but has become important in high-pressure experiments where a 4:1 methanol–ethanol mixture is widely used as a pressure-transmitting medium.[8] In order to determine the nature of the 4:1 mixture at high pressure, it is important to characterize the pure components. No Raman data at high pressure and room temperature have been reported previously for any solid phases of methanol or ethanol. The Raman spectra of methanol and ethanol at pressures up to 100 kbar have therefore been recorded, and the equilibrium pressures of crystallization have been measured.

Experimental Section

Spectroscopic-grade methanol, containing less than 0.08% water (Burdick and Jackson Laboratories, Inc., Muskegon, MI), and absolute ethanol (U.S. Industrial Chemicals Co., New York, NY) were used without further purification.

The samples were compressed in a diamond-anvil cell designed by Mao and Bell.[9] The liquids were contained with a small ruby chip in a hardened steel gasket 0.25–0.4 mm in diameter and approximately 0.15 mm thick, which had been preindented from an original thickness of 0.25 mm. Pressures were calculated from the shift of the ruby R_1 fluorescence line.[10] Diamond anvils cut from low-fluorescent, type-II diamonds, selected by the criteria of Adams and Sharma,[11] were used in the present work. A Spectra Physics Model 164 argon laser operating at 488.0 nm was used as the excitation source. The spectra were recorded at room temperature with a Jobin–Yvon double monochromator (HG-2S) with photon-counting detection.[12] Scattered radiation was collected in the forward direction by a 90° off-axis ellipsoidal mirror.[13]

Polycrystalline samples could sometimes be formed by simply increasing the pressure on the liquid beyond the equilibrium crystallization pressure. Ethanol always crystallized in this way. Methanol could be crystallized by this method but only with difficulty; it usually formed a superpressed liquid. Sometimes crystallization of methanol could be induced by releasing pressure on the glass. Bridgman[14] also reported that ethanol would not superpress and that methanol was difficult to crystallize.

Single birefringent crystals of each alcohol were grown by increasing the pressure on a single nucleation center. This nucleation center was obtained from a polycrystalline sample by releasing the pressure slowly until all but one grain melted, leaving a single grain. The crystallization pressures were measured with one or two crystals in equilibrium with the surrounding liquid and were found to be 35.1 ± 1.0 kbar for methanol and 17.8 ± 1.0 kbar for ethanol. Piermarini et al.[8] reported a value of 35.8 ± 0.8 kbar for the freezing pressure of methanol. Bridgman[15]

0022-3654/80/2084-3130$01.00/0